Dyes and Pigments 92 (2011) 778–782

Contents lists available at ScienceDirect

Dyes and Pigments

journal homepage: www.elsevier.com/locate/dyepig

Naked eye detection of glutathione in living cells using rhodamine B-functionalized gold nanoparticles coupled with FRET

Huai-Hong Cai [a], Hui Wang [a], Jinhui Wang [a], Wei Wei [a], Pei-Hui Yang [a,b,*], Jiye Cai [a,b]

[a] Department of Chemistry, Jinan University, Guangzhou 510632, People's Republic of China
[b] Key Laboratory of Optoelectronic Information and Sensing Technologies of Guangdong Higher Education Institutes, Jinan University, Guangzhou 510632, People's Republic of China

ARTICLE INFO

Article history:
Received 7 April 2011
Received in revised form
9 June 2011
Accepted 9 June 2011
Available online 22 June 2011

Keywords:
Gold nanoparticles
Rhodamine B
Functionalized nanoprobes
FRET
Intracellular glutathione
Colorimetric detection

ABSTRACT

In this study, functionalized gold nanoparticles, in combination with fluorescence resonance energy transfer (FRET), was utilized to visually detect glutathione (GSH) in aqueous samples and then demonstrated its applicability by estimating GSH level in living cells. We first modified the Au NPs with rhodamine B (RB), ON state of FRET, using the electrostatic interaction. In the presence of GSH, the competitive reaction between RB-functionalized nanoprobes (RB-Au NPs) and GSH caused the release of RB molecules from Au NP surface, OFF state of FRET, which was monitored simply by the naked eye. Fluorescence spectra and UV–vis absorption spectra were employed to investigate the spectroscopic characteristics of nanoprobes. Furthermore, the assay conditions, such as nanoprobe concentration, reaction time and the influence of interferent, were investigated. The visible color change of RB-Au NPs solution from dark blue to red in the presence of GSH was observed when the GSH concentration exceeded 10 μM. This one-step naked eye detection depicted here successfully applied for the sensing of human hepatoma (HepG2) intracellular GSH level, showing the potential use in clinical nanodiagnosis. This method allows the rapid colorimetric detection of intracellular GSH without any preliminary treatment and specific instruments.

1. Introduction

Thiols, such as glutathione (GSH), play an important role in the cellular antioxidant defense system [1]. GSH is the most abundant intracellular nonprotein thiols (1–10 mM) [2,3]. It has an important role in maintaining the reducing environment in cells and acts as the redox regulator in redox equilibrium between sulfhydryl and disulfide forms [4–6]. Intracellular GSH levels change dramatically in the response to oxidative stress [1]. Thus, the detection of intracellular GSH is of great importance for investigating cell functions.

Although high-performance liquid chromatography (HPLC) combined with Ellman's reagent (DTNB) is widely used for detecting thiols [7], the method is inconvenient to operate and unsuitable for intracellular thiols detection. Bromobimanes as thiol-labeling fluorescent probes are also non-optimal for intracellular applications owing to bromobimane-induced cell damage [8]. The fluorescent probe recently reported is used in thiols quantification enzyme assays, but this probe suffers from the drawbacks of slight hydrolysis and the difficulty of application *in vivo* [9]. Although great progress in detection intracellular thiols, more effective methods with good sensitivity, selectivity and practicability still need to be developed.

Nanoparticles, especially gold nanoparticles (Au NPs) have been used in variety of detecting molecules because of their unique size and optical properties [10,11]. The color changes associated with the aggregation of Au NPs has led to the development of a number of assays for target species [12,13]. Colorimetric methods can be convenient and attractive in many applications because they can be easily monitored with the naked eyes, without the aid of any advanced instruments [14]. Interestingly, the extinction coefficient of 25 nm-diameter Au NP is $\sim 10^8$ M^{-1} cm^{-1}, several orders of magnitude more than those of traditional organic fluorophores [15]. In addition, among the reported methods for detecting thiols, the use of fluorescent nanoprobes has its apparent advantages in sensitivity. As a result, color changes arising from Au NPs at nanomolar concentrations can be observed by the naked eye, allowing sensitive detection of small amounts of analytes.

Fluorescence resonance energy transfer (FRET) arises from an excited-state energy interaction in which an energy donor transfers energy to an acceptor without photoemission [16]. Accordingly, the

* Corresponding author. Department of Chemistry, Jinan University, Guangzhou 510632, People's Republic of China. Tel./fax: +862085223569.
E-mail address: typh@jnu.edu.cn (P.-H. Yang).

0143-7208/$ – see front matter © 2011 Elsevier Ltd. All rights reserved.
doi:10.1016/j.dyepig.2011.06.016

ON/OFF behaviors of FRET are strongly influenced by the distance between donor and acceptor [17]. Since thiols are used as a competitor in the FRET between energy donor (fluorophores) and energy acceptor (Au NPs) because of the Au–S bonding, the amount of thiol needed for its competition reaction then is typically small. Therefore, the one-step method combining colorimetric characteristics of Au NPs with sensitive measurement of FRET can be used to visually detect trace amounts of thiols.

There has been an increasing demand for the development of simple, cost-effective methodologies in clinical diagnosis. A color change observable by the naked eye in response to the concentration of an analyte can be an indication of quick diagnosis for early warning of disease. Here, we reported naked eye detection of thiols using rhodamine B-functionalized gold nanoparticles (RB-Au NPs) coupled with FRET technique, which is free from any preliminary treatment and specific instruments. We used GSH as a prototype to elucidate colorimetric detection for thiols. Fluorescence spectra and UV–vis absorption spectra were used to investigate spectroscopic characteristics of RB-Au NPs in the absence and presence of GSH that were helpful for better explaining the mechanism of colorimetric detection. We also investigated the selectivity of RB-Au NP nanoprobes and optimized the experiment conditions. This one-step visual assay was further applied in intracellular GSH detection in living cells.

2. Experimental section

2.1. Materials

Chloroauric acid ($HAuCl_4 \cdot 3H_2O$), trisodium citrate dehydrate (98%), RB (98%) and GSH (98%) were obtained from Sigma Aldrich (USA). The chemicals including $Al(NO_3)_3 \cdot 9H_2O$, $FeCl_2 \cdot 4H_2O$, $Mg(NO_3)_2 \cdot 6H_2O$, $Zn(Ac)_2 \cdot 2H_2O$, $CaCl_2 \cdot 2H_2O$, KCl and NaCl were purchased from Sinopharm Chemical Reagent Co., Ltd. (Shanghai, China). All chemicals used were of analytical grade. Mill-water used was purified using a Millipore filtration system (NANOPure, USA) with a resistivity of 18.0 MΩ cm. HepG2 (human hepatoma cell line) were obtained from Sun Yat-Sen University (Guangzhou, China).

2.2. Characterization

Absorption spectra were recorded by a UV-1901 UV–vis spectrophotometer (Beijing, China) using quartz cell with the path length of 1.0 cm. Fluorescent measurements were performed with a 970CRT fluorescence spectrophotometer (Shanghai, China) with a 1.0 cm quartz cell.

2.3. Preparation of Au NPs

Au NPs were synthesized as reported citrate reduction method [18]. Briefly, to a boiling solution of 50 mL of 10 mM $HAuCl_4$, 10 mL of a 1% solution of trisodium citrate dihydrate was added under constant stirring. The color of the solution turned from pale yellow to wine red, indicating that Au NPs was formed. This solution was allowed to react while stirring under heating for 15 min. When the heating mantle was removed, this solution was stirred under room temperature for another 2 h. Finally, Au NPs were purified by centrifugation at 10,000 rpm for 10 min to remove the excess citrate ions.

2.4. Preparation of RB-functionalized Au NPs

Briefly, a 5 ml solution of RB (8.0 μM) was added to the 5 ml of 8.0 nM Au NP solution and allowed to interact for 1 h. Subsequently, RB-functionalized Au NPs were purified by centrifugation for 10 min at 5000 rpm to remove the excess RBs. The concentrations of Au NPs and RB-Au NPs were taken by UV–vis absorption spectra.

2.5. Colorimetric detection of GSH by naked eye

The color change in the RB-functionalized Au NPs on adding predetermined concentrations of GSH was observed by naked eye at room temperature. Briefly, a 3 ml solution of RB-Au NPs at a concentration of 3.0 nM was added to a set of target GSH solutions with a concentration ranging from 0.5 μM to 1000 μM. After 1 h, the color change of RB-Au NP solution in the presence of GSH was observed by naked eye. The experiments about optimization of detecting conditions were carried out under identical conditions. All experiments were repeated three times.

2.6. Cell culture

The human hepatoma (HepG2) cells were cultured (at 37 °C, 50% CO_2) on glass chamber slides in the DMEM growth medium (4.5 g/L glucose with 10% FBS, 1% glutamine, and 1% nonessential amino acids) overnight in a culture box (Heraeus BB16UV). Intracellular expressing fluorescence was detected by flow cytometry. Flow cytometry analysis was performed by a FACSCalibur flow cytometer (Becton Dichinson, USA) with a laser excitation wavelength of 488 nm.

2.7. Naked eye sensing of intracellular GSH

To investigate the feasibility of RB-Au NP nanoprobes in intracellular GSH detection, cell extract experiments were performed to previous methods reported by Choo-Nam Ong et al. [19]. Cells were washed with ice-cold PBS (pH 7.4, 0.10 M) and re-suspended in protein precipitation solution (5% trichloroacetic acid (TCA)–5 mM EDTA). The protein pellet was collected by centrifugation and washed with TCA–EDTA solution. Then the protein was re-dissolved in 3 mL Tris–HCl buffer (pH 7.4, 0.10 M) containing 5 mM EDTA and 0.5% sodium laurylsulfonate (SDS). Aliquots (each 400 μL) were reacted with RB-Au NP nanoprobes (1.5 nM) in Tris–5 mM EDTA buffer (pH 7.4, 0.10 M). Samples were kept in 37 °C for 30 min then the naked eye observation was similar with the above.

2.8. Selectivity of the method

The selectivity of this method was investigated by checking the fluorescent intensity of RB-functionalized Au NPs on the interacting with GSH in the presence of different interference ions, including Al^{3+}, Fe^{2+}, Mg^{2+}, Zn^{2+}, Ca^{2+}, Na^{+}, and K^{+} at the concentrations of 0.1 mM. To confirm the precision and recovery of the nanoprobes, each set of experiments was carried out in triplicate, and similar results within the maximum error of 2–3% were obtained.

3. Results and discussion

3.1. Basic mechanism for visual detection of GSH

We herein used GSH as a prototype to investigate the thiols colorimetric detection by using functionalized nanoprobes. As illustrated in Fig. 1, the optical nanoprobes by design consist of Au NPs conjugated with RBs, which is capable to transferring electron from RBs to Au NPs. As a result, the ON state of FRET is obtained. When the RB-functionalized Au NPs are mixed in a sample solution that contains GSH, RB molecules are released and then the OFF state of FRET is obtained. The gradual release of RB molecules will

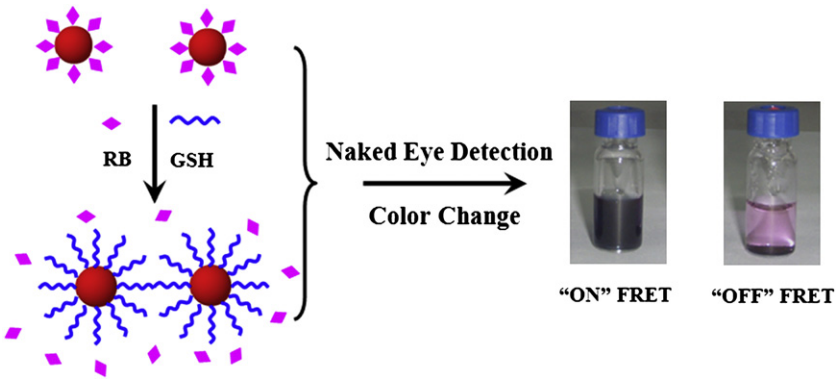

Fig. 1. Schematic illustration of a homogenous detection of thiols using RB-functionalized Au NP nanoprobes coupled with FRET.

deepen the color change of the whole nanoparticle population, which can be detected by naked eye. The color changes of the supernatant can then be correlated to the target GSH concentrations. A higher target GSH concentration lead to more extensive release of RBs and then deep red color was observed.

3.2. Naked eye detection of GSH by RB-Au NP nanoprobes

Au NPs with particle size of 25 nm were synthesized and the solution was wine-red (Fig. 2, left). Upon conjugation with RBs, the color of RB-modified Au NP solution was subsequently dark blue, which was ascribed to the color mixture between higher concentrations of RBs and Au NPs (Fig. 2, middle). The RB-functionalized Au NP solution has some aggregation, which was due to the decreased repulsive interactions between higher concentrations of RB-Au NPs. When GSH was added, the color changes of RB-Au NP solution turned to red. After centrifugation, the supernatant become clear red, accompanying with the appearance of precipitate (Fig. 2, right). A higher target GSH concentration led to deepen red in solution, which resulted from more extensive release of RB molecules from Au NP surface. This shows that RB-Au NP nanoprobes have a good recognition for thiols. The color change of RB-Au NPs in the presence of GSH is ascribed to competitive interactions because of the Au–S bonding. Because the process of RBs release from fluorescent nanoprobes can be monitored visually, the naked eye alone can judge the presence or absence of thiols without the aid of any instruments.

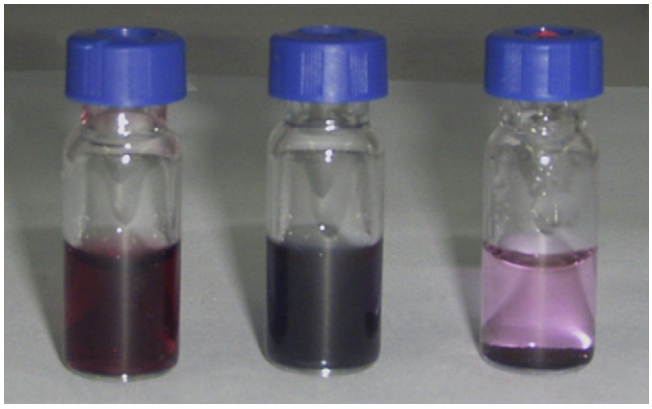

Fig. 2. Colors of Au NPs (left), RB-functionalized Au NPs (middle), and RB-Au NPs on reacting with >1 mM GSH (right). (For interpretation of the references to color in this figure legend, the reader is referred to the web version of this article.)

We further used fluorescent spectra and UV–Vis absorption spectra to explain the mechanism of colorimetric detection of GSH. As shown in Fig. 3, the fluorescent intensity of RB-Au NPs was almost near to zero. However, fluorescent intensity of RB-Au NPs enhanced with increasing GSH concentrations, indicating that RBs were released from Au NPs basing on specific Au–S bonding. Fig. 4 is the UV–vis absorption spectra of RB-Au NP nanoprobes before and after addition of GSH. The Au NP solution was wine red with an SPR band at 520 nm. Upon functionalization of RBs, the SPR band of RB-Au NP solution was little broadened. In the presence of GSH, a new band at 580 nm and a new broadening of the SPR occurred. The band at 580 nm was consistent with the characteristic band of RB, demonstrating that RBs released from Au NPs because of competitive binding. The new broadening of the SPR at 680 nm indicated that GSH induced Au NPs aggregation. This result showed that color changes associated with the aggregation of Au NPs induced by GSH binding can be exploited for developing a colorimetric sensor for GSH detection.

To evaluate the minimum concentration of GSH in aqueous solution detectable by this color changes, we added 3.0 nM RB-Au NP nanoprobes into different concentrations of GSH solution with 1000 μM, 500 μM, 100 μM, 50 μM, 10 μM, 1 μM, and 0.5 μM, respectively. With increased concentration of target GSH, the red of the supernatant deepened accordingly (Fig. 5). After centrifugation, the results showed that only when [GSH] ≥ 10 μM, were the red changes of color in supernatant obvious, whereas when

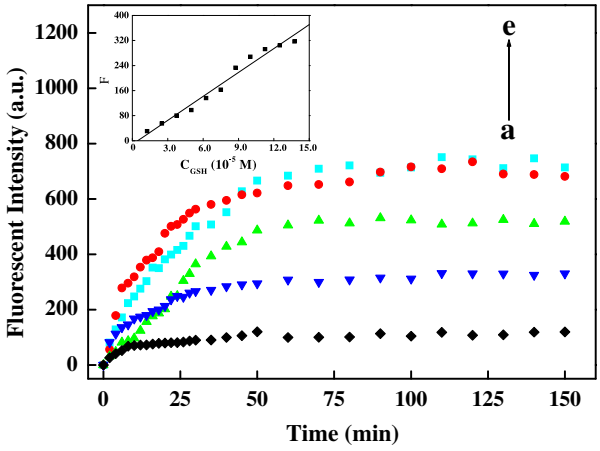

Fig. 3. Effects of GSH concentrations and reaction time on the fluorescent intensity of RB-Au NPs. Curves from (a) to (e) correspond to 50 μM, 100 μM, 500 μM, 1000 μM, and 5000 μM GSH. Fluorescence intensities were measured at 578 nm. The concentration of RB-Au NPs was 3.0 nM. Inset of Fig. 3, calibration curve of fluorescent intensity vs. GSH concentration was provided.

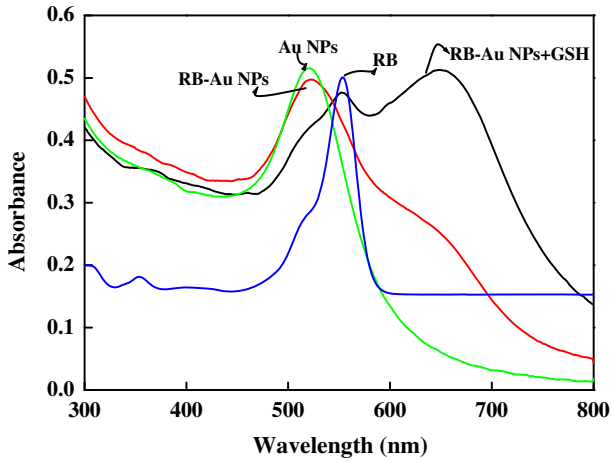

Fig. 4. UV–Vis absorption spectra of Au NPs, RB, RB-Au NPs, and RB-Au NPs in the presence of GSH.

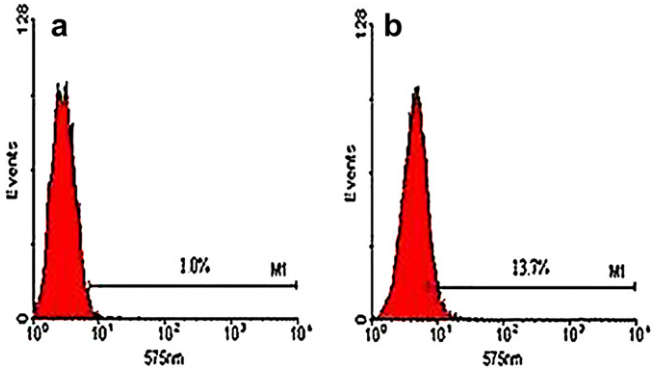

Fig. 6. Flow cytometry analysis of fluorescent signals in cells before (a) and after (b) incubation with RB-Au NPs.

[GSH] $<$ 10 μM, distinct changes of the solution could not be observed. We also tested the effects of either increasing or decreasing the concentration of RB-Au NPs in the solutions, but were unable to detect lower concentrations of GSH. A correlation can be established between the red color deepening of the whole nanoparticle population and the increasing concentrations of target GSH (Fig. 5). We therefore concluded that the minimum concentration of GSH detectable by naked eye was approximately 10 μM.

Although Chang et al. [20] demonstrated a similar level of sensitivity and selectivity for GSH detection as our assay, however, the acid detection condition was unsuitable for intracellular applications owing to acid-induced cell damage. In contrast, the physiologically relevant environments and optimal experiment conditions used in our assay are suited for the application in clinical diagnosis. The lowest detectable concentration cannot be compared with that obtained with the help of advanced instruments, but we believe, however, that this concentration sets the record for the detection of GSH by the naked eye alone.

3.3. Optimal experiment conditions

To further obtain sensitively colorimetric detection in GSH level of cell sample, the assay conditions, such as RB-Au NP nanoprobe concentration, reaction time, and the influence of interferent, were investigated by the fluorescence spectra.

RB-Au NP concentrations affect the recognition capacity of nanoprobes, correspondingly, influences the sensitivity of detection. As nanoprobe concentrations increased, fluorescent intensity enhanced, demonstrating that RB-Au NPs have a good recognition for GSH. This indicates that higher concentrations of nanoprobes can accommodate more RB molecules for GSH bonding, and thus lead to clear observation the color changes by naked eye. Therefore, in order to enhance detection sensitivity and reduce background interference, 3.0 nM of RB-Au NPs was chosen as the optimal nanoprobe concentration for visual capturing GSH.

The influence of reaction time on naked eye detection was investigated by monitoring the fluorescent intensity of RB-Au NPs in the presence of GSH. When the reaction time was increased, the fluorescent intensity of RB-Au NPs increased initially and then tended to be stable at the reaction time more than 1 h (Fig. 3). Therefore, the 1-h time course was introduced to record nanoprobe-based OFF/ON FRET in this colorimetric detection.

Furthermore, the influences of coexisting substances were investigated. We tested the selectivity of this assay for GSH by using some metal ions as the interferent, including Al^{3+}, Fe^{2+}, Mg^{2+}, Zn^{2+}, Ca^{2+}, Na^{+}, and K^{+} at the concentrations of 0.1 mM. None obvious color changes of RB-Au NPs solution could be observed even after one day, indicating that the interferential ions have little influence on thiols detection. Interference from amines, amino acids, and certain thiols and proteins is minimal. Inset of the Fig. 3, a qualitative detection of GSH was provided. Under optimal experiment conditions, the calibration plot exhibited a good detection range from 12 μM to 1384 μM of GSH ($F = -11.28 + 25.47\ C_{GSH}$; correlation coefficient, $r = 0.9879$), with a detection limit of 1.0 μM. The nanoprobe-based colorimetric detection has good selectivity and can be applied to measure intracellular thiols level.

3.4. GSH visual detection in cell samples

It is well-known that GSH is the most abundant intracellular nonprotein thiols (1–10 mM) [2,3]. In the cell sample, the competitive reaction between RB-Au NP nanoprobes and GSH or other protein thiols is existed. Higher concentrations of GSH can preferentially bind with RB-Au NPs because of the concentrations-based competitive binding. Lower concentrations of other thiols then have less change to bind with nanoprobes. Therefore, RB-Au

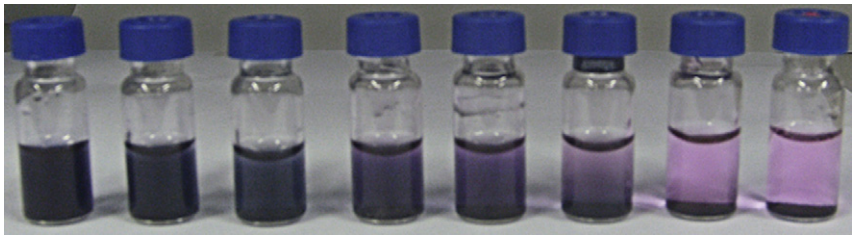

Fig. 5. A photography of RB-Au NP solution in the presence of different concentrations of GSH with 0 (a), 0.5 μM (b), 1.0 μM (c), 10 μM (d), 50 μM (e), 100 μM (f), 500 μM (g), and 1000 μM (h) from left to right.

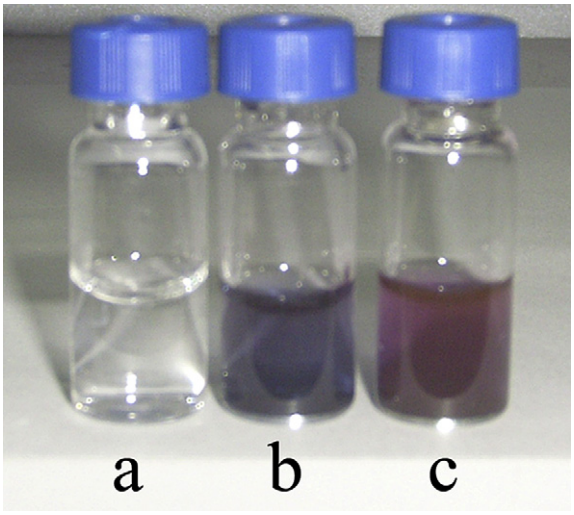

Fig. 7. Colors of cell extracts (left), RB-functionalized Au NPs (middle), and cell extracts in the presence of RB-Au NPs (right). (For interpretation of the references to color in this figure legend, the reader is referred to the web version of this article.)

NPs can be used as optical nanoprobes to visually estimate intercellular GSH level by naked eye.

Normal hepatocytes conserve high levels of GSH. However, liver injury caused oxidative stress can induce depletion of GSH and then serve decline in concentrations of other protein thiols [21]. To test this method in cellular GSH detection, flow cytometry was first used to characterize the fluorescent signals of HepG2 cells in the presence of RB-Au NP nanoprobes. In a negative control, only 1% fluorescence could be detected, which was due to the autofluorescence of cells (Fig. 6, curve a). However, when cells were incubated with RB-Au NPs (3.0 nM) for 2 h, intracellular fluorescence increased to 13.7% (Fig. 6, curve b). This result indicates that the optical nanoprobes are membrane-permeable, and the increasing cell expressing fluorescence is due to the release of RBs from optical nanoprobes basing on intercellular GSH binding. To further apply this method in cell sample, the intercellular GSH level in cell extracts were observed by naked eye. After being incubated with RB-Au NP nanoprobes for 30 min, the supernatant solution of cell extracts showed a clear red (Fig. 7). Rather than quantitative estimation, it seems that the method provides a quick qualitative estimating of samples. It was apparent from Fig. 5 that a concentration of 1.0 mM thiols showed a visible color change of the solution, which concluded that the thiols content of the cells was >1.0 mM. This demonstrates the feasibility of extending the method for the estimation of GSH level in real cell samples. The naked eye detection method discussed here can be applied in early warning, quick detection and treatment evaluation of disease.

4. Conclusion

We devised a simple method for the visual detection of GSH in cells using RB-functionalized Au NPs. This novel RB-Au NPs coupled with FRET design offers many advantages, including simplicity of preparation and without specific instruments. The color of RB-Au NP solution was found to change from blue to red in the presence of 10 μM GSH, which was supported by the results of fluorescence spectra, UV–vis absorption spectra, and flow cytometry analysis. A good correlation was obtained between the red color deepening of the whole nanoparticle solution and the increasing concentrations of target GSH. This assay was then successfully applied to the colorimetric detection of intracellular GSH in living cells with good sensitivity. The color change observable by the naked eye can advantageously be used for a preliminary screening without the aid of any advanced instruments. The ability to detect the presence of intercellular GSH can be potentially extended to facilitate miniaturization for "lab-on-a-chip" and related applications in nanodiagnosis.

Acknowledgment

This work was supported by grants from the Major State Basic Research Development Program of China (973 Program) (No. 2010CB833603), National Natural Science Foundation China (No. 21071064), the Key Project of Chinese Ministry of Education (No. 210254), the Fundamental Research Funds for the Central Universities (Nos. 21609305 and 21610427), Specialized Research Fund for the Doctoral Program of Higher Education (No. 20104401120004) and the Innovation Fund of the "211 Project" for Biomaterials and Tissue Engineering of Jinan University.

References

[1] Zhang SY, Ong CN, Shen HM. Critical roles of intracellular thiols and calcium in parthenolide-induced apoptosis in human colorectal cancer cells. Cancer Lett 2004;208:143–53.
[2] Wang CH, Sinskey AJ, Lodish HF. Oxidized redox state of glutathione in the endoplasmic reticulum. Science 1992;257:1496–502.
[3] Hong R, Han G, Fernández JM, Kim BJ, Forbes NS, Rotello VM. Glutathione-mediated delivery and release using monolayer protected nanoparticle carriers. J Am Chem Soc 2006;128:1078–9.
[4] Rahman I, MacNee W. Regulation of redox glutathione levels and gene transcription in lung inflammation: therapeutic approaches. Free Radic Bio Med 2000;28:1405–20.
[5] Pullela PK, Chiku T, Carvan MJ, Sem DS. Fluorescence-based detection of thiols in vitro and in vivo using dithiol probes. Anal Biochem 2006;352:265–73.
[6] Meister A, Anderson ME. Glutathione. Annu Rev Biochem 1983;52:711–60.
[7] Komuro C, Ono K, Shibamoto Y, Nishidai T, Takahashi M, Abe MJ. Rapid and simple method for quantitative determination of non-protein sulphydryls in mouse liver by reversed-phase high-performance liquid chromatography. J Chromatogr 1985;338:209–12.
[8] Kamencic H, Lyon A, Paterson PG, Juurlink BHJ. Monochlorobimane fluorometric method to measure tissue glutathione. Anal Biochem 2000;286:35–7.
[9] Maeda H, Matsuno H, Ushida M, Katayama K, Saeki K, Itoh N. 2,4-dinitrobenzenesulfonyl fluoresceins as fluorescent alternatives to ellman's reagent in thiol-quantification enzyme assays. Angew Chem Int Edit 2005;44:2922–5.
[10] Leng B, Zou L, Jiang J, Tian H. Colorimetric detection of mercuric ion (Hg^{2+}) in aqueous media using chemodosimeter-functionalized gold nanoparticles. Sensor Actuat B-Chem 2009;140:162–9.
[11] Leng B, Jiang J, Tian H. A mesoporous silica supported Hg^{2+} chemodosimeter. AIChE J 2010;56:2957–64.
[12] Mirkin CA, Letsinger RL, Mucic RC, Storhoff JJ. A DNA-based method for rationally assembling nanoparticles into macroscopic materials. Nature 1996;382:607–9.
[13] Wei X, Qi L, Tan J, Liu R, Wang F. A colorimetric sensor for determination of cysteine by carboxymethyl cellulose-functionalized gold nanoparticles. Anal Chim Acta 2010;671:80–4.
[14] Guo Z, Zhu W, Zhu M, Wu X, Tian H. Near-infrared cell-permeable Hg^{2+}-selective ratiometric fluorescent chemodosimeters and fast indicator paper for $MeHg^{+}$ based ontricarbocyanines. Chem Eur J 2010;16:14424–32.
[15] Jin R, Wu G, Li Z, Mirkin CA, Schatz GC. What controls the melting properties of DNA-linked gold nanoparticle assemblies? J Am Chem Soc 2003;125:1643–54.
[16] Kim JS, Quang DT. Calixarene-derived fluorescent probes. Chem Rev 2007;107:3780–99.
[17] Patolsky F, Gill R, Weizmann Y, Mokari T, Banin U, Willner I. Lighting-up the dynamics of telomerization and DNA replication by CdSe–ZnS quantum dots. J Am Chem Soc 2003;125:13918–9.
[18] Fens G. Controlled nucleation for the regulation of the particle size in monodisperse gold suspensions. Nature 1973;242:20–2.
[19] Yang CF, Shen HM, Ong CN. Ebselen-induces apoptosis in HepG2 cells through rapid depletion of intracellular thiols. Arch Biochem Biophys 2000;374:142–52.
[20] Chen SJ, Chang HT. Nile red-adsorbed gold nanoparticles for selective determination of thiols based on energy transfer and aggregation. Anal Chem 2004;76:3727–34.
[21] Han D, Hanawa N, Saberi B, Kaplowitz N. Mechanisms of liver injury. III. Role of glutathione redox status in liver injury. Am J Physiol-Gastr L 2006;291:G1–7.